Multi-resolution heterogeneity analysis of urban flows

Jingzi Huang[1*] and Maarten van Reeuwijk[1]
[1]Department of Civil and Environmental Engineering,
Imperial College London, London SW7 2AZ, UK
[*] E-mail: jingzi.huang17@imperial.ac.uk

ABSTRACT
Whether or not urban form or urban flow is perceived to be heterogeneous is dependent on the measurement resolution. In this study, we construct flow fields at various resolutions via a coarse-graining operation using a square spatial convolution filter. We use these fields to explore multi-scale aspects of heterogeneity with the aim preparing for developing scale-aware parameterisations for numerical weather prediction (NWP). The case we studied involves neutral flow around a staggered array of cubes with random heights. We coarse-grain the Reynolds-averaged velocity $\overline{u}$ using seven different filter lengths to analyse the filtered velocity field at these different resolutions. By exploring the multi-resolution properties of these fields, for example, by examining the tile-based variances (which represent the heterogeneity) as a function of the resolution at different heights, we highlight that the conventional spatially averaged value is not representative to describe the high-resolution field.

1. INTRODUCTION

Heterogeneity represents spatial variation and is dependent on the measurement resolution. Higher resolution would provide more detailed information about urban surface properties but would also require more computational resources [1, 2]. It can be quantified by measuring the variance of a system property [3]. The current numerical weather prediction (NWP) is usually interested in the spatially average of properties over an entire horizontal plane, ignoring the variance within the plane. This is a concession primarily because that the current resolution equipped in the NWP is of $O(1\ \mathrm{km})$, which is not able to resolve all the details especially within the canopy region [4]. Indeed, in the canopy region, the heterogeneity and variance are apparent [5, 6], so that the spatial average becomes less representative. Therefore, understanding the heterogeneity evolves with the resolution is important and would be benefit to the parameterisations of the unresolved parts in the numerical simulation under different resolutions.

In the present study, a Multi-Resolution framework is used to analyse heterogeneity. In the Multi-Resolution framework, starting from an original-resolution field, a series of low-resolution fields is obtained through a coarse-graining operation, which reduces the resolution by a factor of two using spatial average in a square filter. Then, the heterogeneity of the resolved and unresolved fields at different resolutions is explored. The paper is organized as follows: Sect. 2 introduces the background equations and simulation details; Sect. 3 provides the results showing how the velocity field evolves with the different resolutions and Sect. 4 remarks on the conclusions.

2. METHODOLOGY AND NUMERICAL DETAILS

Inspired by the volume-averaging framework of [7, 8], and considering that in numerical weather predications, the computational cells are much wider than they are high, particularly near the surface, we employ a two-dimensional superficially area-averaging framework by defining a two-dimensional masking function $\mathcal{A}(\boldsymbol{x}_\perp)$ as the area averaging kernel on the horizontal x-y plane with the area A, the masking function is 1 within the averaging domain and 0 outside of it, with this notation, the superficial (area) average of an arbitrary scalar $\varphi(\boldsymbol{x})$ is given as

$$\tilde{\varphi}(\boldsymbol{x}) = \frac{1}{A}\int_{\Omega} \mathcal{A}(\boldsymbol{x}_\perp - \boldsymbol{y}_\perp)\varphi_f(\boldsymbol{y}_\perp, z)\,\mathrm{d}\boldsymbol{y}_\perp\,, \tag{1}$$

where $\Omega(\boldsymbol{x})$ is the whole domain of interest, however, only the scalar within its fluid subdomain is integrated, e.g., $\varphi_f(\boldsymbol{x})$.

Then, we define the superficially spatial average over the entire x-y plane whose area is A_T

$$\langle\cdot\rangle = \frac{1}{A_T}\int_{\Omega_f} \cdot\,\mathrm{d}A\,, \tag{2}$$

and note that $\langle\varphi\rangle = \langle\tilde{\varphi}\rangle$. Hereafter, we refer to $\varphi(\boldsymbol{x})$ as the 'original' field and $\tilde{\varphi}(\boldsymbol{x}, L)$ as the 'filtered' field.

The case we studied involves neutral flow around a staggered array of cubes with random heights, where the width and mean height are both $h_m = 10$ m [6]. The case was simulated using uDALES, an open-source large-eddy simulation model for urban environments [9]. Periodic lateral boundary conditions are used, with a free-slip boundary condition at the top. The flow is forced by a constant kinematic pressure gradient $\mathcal{F}_u = 4.1912 \times 10^{-3}\ \mathrm{ms}^{-2}$. The domain size is $L_x \times L_y \times L_z = 16h_m \times 16h_m \times 10h_m$, and the number of grid cells is $N_x \times N_y \times N_z = 256 \times 256 \times 256$. The initial velocity profile is uniform. In this study, the averaging kernel $\mathcal{A}$ is a square with the lengths of $L = 1.25\ \mathrm{m}, 2.5\ \mathrm{m}, 5\ \mathrm{m}, 10\ \mathrm{m}, 20\ \mathrm{m}, 40\ \mathrm{m}, 80\ \mathrm{m}$, respectively.

DOI 10.5258/WES/P0041

3. RESULTS

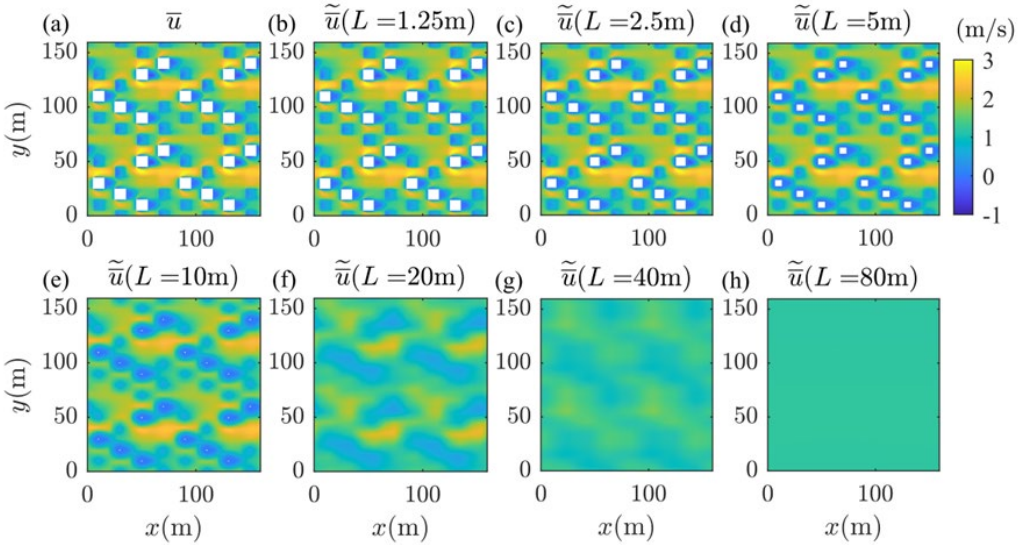

Figure 1, The horizontal plane of Reynolds-averaged velocity $\overline{u}$, (a) with the original resolution of the simulation, (b-h) spatial averaged under different filter lengths, at the mean building height level $h_m = 10\ m$. The white boxes represent the building.

To note the building area (solid subdomain), we define a solid indicator $\varepsilon(\boldsymbol{x})$ which is 1 only at the building area and 0 anywhere else. Substituting $\varphi = \varepsilon$ and $\overline{u}$ into the spatial average Eq.1, we obtain the filtered field for the building $\tilde{\varepsilon}(\boldsymbol{x})$ and for the fluid velocity $\widetilde{\overline{u}}(\boldsymbol{x})$ with different filter lengths (resolutions), which are shown in figure 1. First, the filtered building area $\tilde{\varepsilon}$ can range between 0 to 1 depending on the location of the filter, note that, $\tilde{\varepsilon} = 1$ only when the whole filter emerges within the building area, in which case the filtered velocity $\widetilde{\overline{u}}$ does not exist. Therefore, in this field figure, only the loci ε (or $\tilde{\varepsilon}$) is 1 are labelled as white boxes to remark the absence of the velocity. With the increase of the filter length, the area of these white boxes gets smaller and finally vanishes in the large filter length, which indicates that for the low resolution, the building and its relevant properties, e.g., the drag force, are not resolved and will induce the uncertainties to the flow dynamics.

Second, figure 1 shows the Reynolds-averaged wind velocity $\overline{u}$ from its original resolution (figure 1a) to its filtered average $\widetilde{\overline{u}}$ with different filter lengths (figures 1c-h) at the mean building height $h_m = 10$ m. As expected, the figures clearly show that as the filter length grows (i.e., the resolution decreases), the fluid velocity field becomes more homogeneous, less variance and heterogeneity can be observed, indicating that more information becomes unresolved.

To quantify the heterogeneity in a field, we are interested in the between-cell variance $V_\varphi(z, L)$, over the horizontal plane, which is defined as

$$V_\varphi(z, L) = \frac{1}{L_x L_y} \iint \left(\varphi(\boldsymbol{x}, L) - \langle\varphi\rangle(z, L)\right)^2 \mathrm{d}x\mathrm{d}y\,. \tag{3}$$

Substituting $\varphi = \overline{u}$ and $\widetilde{\overline{u}}$, we obtain this between-cell variance of the streamwise velocity varying with filter lengths and plot it with the averaged streamwise velocity $\langle\widetilde{\overline{u}}\rangle$ (or $\langle\overline{u}\rangle$, they are identical) in the figure 2. To show the variance clearly, the plot is only restricted within the canopy region (reminding that, the maximum building height is $1.8h_m$), above the canopy region, not shown here, we observe very small variances for all the filter lengths, and the averaged velocity profiles gradually fits the log-law.

Figure 2 shows that horizontal slab averaged velocity $\langle\widetilde{\overline{u}}\rangle$ and $\langle\overline{u}\rangle$ are independent of the filter lengths. However, as the filter length gets smaller (i.e., the resolution gets higher, looking from figures 2h to 2a), the velocity variance $V_{\widetilde{\overline{u}}}$ becomes significant, and it suggests that for high resolutions, e.g., figures 2(a, b), the average is unlikely to represent the detailed distribution of the velocity field. Among the low resolutions, for example, from figures 2h to 2f, even if we increase the resolution by a factor of 4, the variance remains very low, indicating that the heterogeneity it captures is still not ideal. This indicates that for the current NWP (usually has a low resolution of $O(1\ \text{km})$), our attempt to increase the resolution may not induce a significant improvement.

Therefore, to investigate how the variance evolves with the resolution, we plot the between-cell variance of the filtered (resolved) velocity $V_{\widetilde{\overline{u}}}$ at four specific heights against different filter lengths, for a comparison we also plot the variance on the original velocity field $V_{\overline{u}}$ which is independent of resolution. On the other hand, we denote an unresolved velocity $\overline{u}'''(\boldsymbol{x}, L) = \overline{u}(\boldsymbol{x}) - \widetilde{\overline{u}}(\boldsymbol{x}, L)$, and also calculate and plot the variance within the unresolved

DOI 10.5258/WES/P0041

velocity field $V_{\overline{u}}'''$, as shown in figure 3, and by definition $V_{\overline{u}} = V_{\widetilde{\overline{u}}} + V_{\overline{u}}'''$. We are also interested in the tile-based variance $\Delta V_{\widetilde{\overline{u}}}(\boldsymbol{x}, L)$ --- the tile-based variance represents the change of the between-cell variance between the two neighbour resolutions, e.g., $\Delta V_{\widetilde{\overline{u}}}(5\ m) = V_{\widetilde{\overline{u}}}(10\ \mathrm{m}) - V_{\widetilde{\overline{u}}}(5\ \mathrm{m})$.

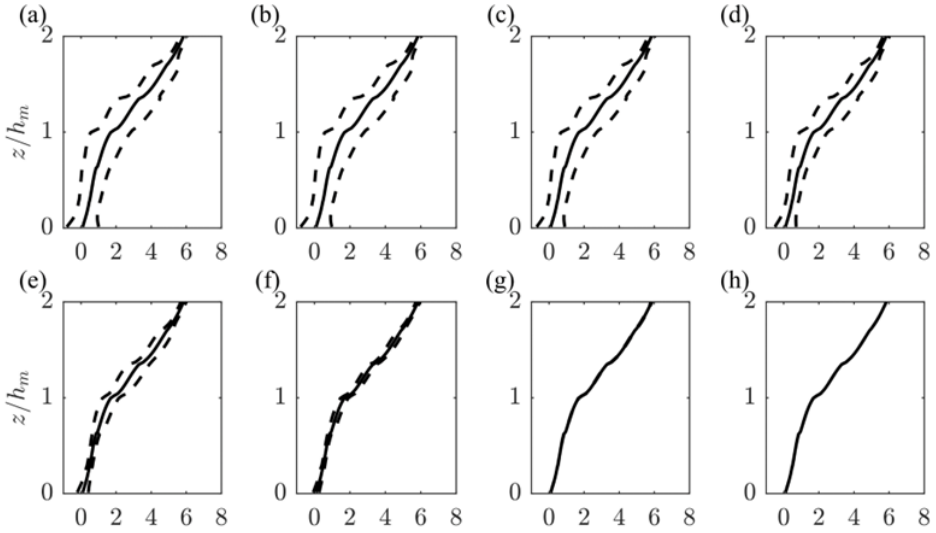

Figure 2, (a-g) The slab averaged filtered velocity $\langle\widetilde{\overline{u}}\rangle$ (solid line), varying with the filter length for filter length L = {1.25, 2.50, 5, 10, 20, 40, 80} m, *respectively, (h) is the slab averaged velocity in the original field. The dashed lines mark the upper and lower bound of the variance around the average, i.e., $\langle\widetilde{\overline{u}}\rangle \pm V_{\widetilde{\overline{u}}}$. The height is only shown up to the canopy region.*

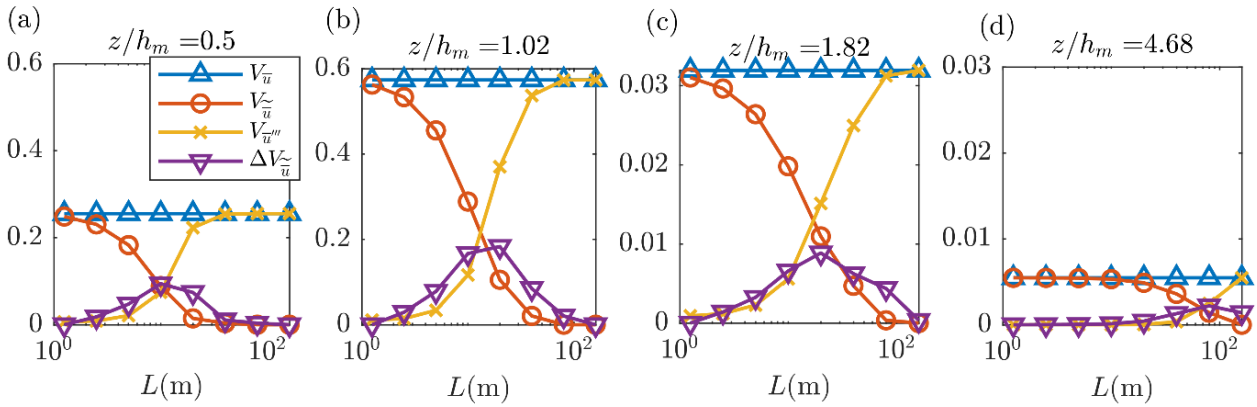

Figure 3, The between-cell variance of the original velocity $V_{\overline{u}}$, the filtered (resolved) velocity $V_{\widetilde{\overline{u}}}$ and the unresolved velocity $V_{\overline{u}}'''$ and the tile-based variance of the resolved velocity $\Delta V_{\widetilde{\overline{u}}}$, evolving with the filter length at four different heights.

In terms of the variance of original velocity field $V_{\overline{u}}$, the figure shows that, in the canopy region (figures 3a-c), $V_{\overline{u}}$ at the mean building height (figure 3a) is relatively larger than that at the half mean-building height and the maximum building height (figures 3b and 3c, respectively), which is primarily due to the morphology change. However, in the roughness sublayer, $V_{\overline{u}}$ becomes much smaller due to the absence of the building. The variance is expected to be even closer to zero above in the inertial sublayer. In terms of the resolved and unresolved velocities, the figure shows that, in the canopy region, with the filter length grows (resolution lows), the variance of the resolved velocity $V_{\widetilde{\overline{u}}}$ decreases and that of the unresolved velocity $V_{\overline{u}}'''$ increases --- again reassure that in the lower resolution, more information becomes unresolved instead of being resolved. However, in the roughness sublayer, the variances seem less sensitive to the change of filter length, indicating that the no-building region has a lower requirement on the resolution than the building region (e.g., canopy region).

The tile-based variance of the filtered velocity field $\Delta V_{\widetilde{\overline{u}}}$, represents the proportion of between-cell variance that becomes resolved by increasing the resolution. Figures 3(a-c) show this variance as a function of the filter length,

DOI 10.5258/WES/P0041

which peaks around the length $10\ \mathrm{m} - 20\ \mathrm{m}$ implying that there is a significant increasing unresolved part when the resolution changes over $10\ \mathrm{m} - 20\ \mathrm{m}$. Note that this filter length is roughly where the variances of resolved and unresolved between-cell variance cross over. Practically, this change suggests that, for low resolution for example $L = 80\ \mathrm{m}$, the effort should be made to at least increase the resolution by approximately 8 times (to $L = 10\ \mathrm{m}$), to have a practically significant improvement.

4. CONCLUSIONS

A Large-Eddy simulation was performed over a staggered array of cubes with random heights and the heterogeneity was investigated by a multi-resolution analysis. The variances of the streamwise velocity fields showed that, in the canopy region, although the resolutions do not affect the horizontally spatial averaged velocity over the plane, the higher the resolution, the more heterogeneity, making the averaged velocity become less representative. The variances also indicated that, in the relatively low resolution that is used in NWP, much information is unresolved which needs to be modelled. For example, we observed that the building (solid) part is not resolved in the low resolutions, which suggested that the drag of the building is not captured. As drag plays an important role in wind momentum, developing a numerical model that considers heterogeneity could be a future work.

ACKNOWLEDGEMENTS.

The support of the ARCHER2 UK National Supercomputing Service (project ARCHER2-eCSE05-3) and the NESRC highlight grant ASSURE: Across-Scale ProcesseS in Urban Environment (NE/W002868/1) is acknowledged.

DECLARATION OF INTERESTS.

The authors report no conflict of interest.

REFERENCES

[1] Cadenasso ML, Pickett STA & McGrath B. (2013). “Ecological heterogeneity in urban ecosystems: reconceptualized land cover models as a bridge to urban design. In: Pickett STA, Cadenasso ML and McGrath B (eds)”. *Resilience in Ecology and Urban Design: Linking Theory and Practice for Sustainable Cities*. Dordrecht: Springer, pp. 107–129.

[2] Cadenasso ML, Pickett STA & Schwarz K. (2007). “Spatial heterogeneity in urban ecosystems: reconceptualizing land cover and a framework for classification”, *Frontiers in Ecology and the Environment* 5: 80–88.

[3] Fitch PJR, Lovell MA, Davies SJ. (2015). “An integrated and quantitative approach to petrophysical heterogeneity”, *Marine and Petroleum Geology*. **63**, 82–96.

[4] Sutzl B.S., Rooney G.G. & van Reeuwijk, M. (2020). “Drag distribution in idealized heterogeneous urban environments”, *Boundary-Layer Meteorology.* **178**, 225–248.

[5] Coceal O, Thomas TG & Belcher SE. (2007). “Spatial variability of flow statistics within regular building arrays”, *Boundary-Layer Meteorology*. **125**, 537–552.

[6] Xie Z.-T. & Castro I. P. (2008). “Efficient generation of inflow conditions for large eddy simulation of street-scale flows”, *Flow, turbulence and combustion*, **81**, 449–470.

[7] Whitaker S. (1999). “The method of volume averaging”, *Theory and applications of transport in porous media*, Kluwer Academic Publishers.

[8] Schmid M., Lawrence G.A., Parlange M.B. & Giometto M.G. (2019). “Volume averaging for urban canopies”, *Boundary-Layer Meteorology.* **173**, 349–372.

[9] Owens S. O., Majumdar D., Wilson C. E., Bartholomew P., & van Reeuwijk M. (preprint). “A conservative immersed boundary method for the multi-physics urban large-eddy simulation model uDALES v2.0”, *EGUsphere*

DOI 10.5258/WES/P0041